2014 American Control Conference (ACC)
June 4-6, 2014. Portland, Oregon, USA

On the Warmup of Li-ion Cells from Sub-zero Temperatures

Shankar Mohan†*, Youngki Kim†, Anna G. Stefanopoulou† and Yi Ding‡

Abstract— **Lithium (Li) ion cells suffer from significant performance degradation at sub-zero temperatures. This paper presents a Predictive Control based technique that exploits the increased internal resistance of Li-ion cells to improve the power capability of Li-ion cells operating at sub-zero temperatures. The current is shaped as bi-directional pulses to minimize total energy discharge and adverse side reactions. The magnitude of current is determined by solving an optimization problem that penalizes energy loss. The penalty in energy loss is found to be influence the size external storage elements. When compared with the case when no penalty is imposed, gains of up to 20% are noted through simulations.**

I. Introduction

The use of high energy density rechargeable battery technologies has recently enjoyed widespread adoption in consumer electronics and automotive/aerospace applications. The archetype of rechargeable technology, Li-ion batteries, has over the last decade benefited from improvements in material science through increased energy and power density. Li-ion batteries, although widely adopted, suffer significant performance degradation at low temperatures ($\leq -10^o$C) posing a challenge for automotive applications. It is well documented that at low temperatures, the discharge capability of Li-ion cells can be less than 70% of that at room temperature [1]; for it has been proposed that the reduction in electrode and electrolyte diffusivity [2], decrease in reaction kinetics [2] and loss of available lithium owing to plating and absorbtion into the Solid Electrolyte Interface (SEI) layer [3] are the most likely reasons.

Although improvement to sub-zero performance through changes to design and construction of cells [4] have been pursued, the need for fast warm-up is relevant for existing equipments. Battery warm-up techniques can be broadly classified as – (1) jacket/resistive/external heat-up (2) internal heating using high-frequency currents [5]. Ji *et al.* in [6] compare different heating strategies and conclude that for Li-ion cells, internal heating is more effective than using external heating elements if no external power source is utilized, a scenario we term as *standalone* and is of consideration in this paper.

Most techniques discussed in literature strive to warm the cell until a certain pre-specified cell temperature is reached. Since in most applications, the cell serves as a source of power, in this work, we use the cell's pulse power capability, instead of the temperature, as a condition to terminate the warm-up operation. Consequently, we seek to investigate the feasibility of increasing the power capability in an energy efficient manner.

Power capability is an estimated quantity whose accuracy is determined by the fidelity of the model that captures the electrical dynamics of the cell. Modeling the electrical behaviour of Li-ion cells at sub-zero temperatures, particularly at high current rates, is more challenging than emulating its thermal dynamics [7]. Thus, owing to the inherent relation between operating temperature and power capability, in this paper, temperature rise is taken as a measurable surrogate. Then, the stated objective of increasing power capability can be re-written as one of effecting temperature rise in an energy conscious manner until the desired power can be delivered.

Maximizing temperature rise while regulating energy lost provides for certain desirable characteristics of the battery current. Heat generated being proportional to the root-mean-square (rms.) of input current, it follows that the candidate current profile be bi-directional to minimize cumulative discharge and achieve fast warm-up. Drawing bi-directional currents necessitates that a temporary energy reservoir for energy shuttling, such as an ultra-capacitor, be available. Since the bi-directional current includes a charging phase, it is important to note that charging the cell at low temperatures is challenging and needs some consideration.

Charging Li-ion cells at subzero temperatures is difficult because of the reduced diffusivity in the anode that results in increased polarization and a drop in electrode overpotential. From a control perspective, the propensity of charging currents to cause plating can be minimized by actively regulating the electrode overpotential. In this paper, the anode polarization is indirectly controlled by enforcing the magnitude of charging currents to be less than the discharging portion of the pulse.

This paper attempts to study the feasibility of using computationally efficient models to improve the power capability of Li-ion cells in an energy efficient manner. This paper is organized as follows. The models that are used to mimic the cell's electrical and thermal behavior are detailed in Section II. The control problem is formulated in Section III and an example simulation is studied in Section IV. Conclusions and final remarks are made in Section V.

II. Modeling

This section introduces the models of electrical and thermal dynamics adopted in this study. The validity of the chosen models for the application at hand is ascertained through experimental validation.

The author is with † the University of Michigan, Ann Arbor;
‡ U.S. Army Tank Automotive Research, Development and Engineering Center (TARDEC)
*e-mail: elemsn@umich.edu

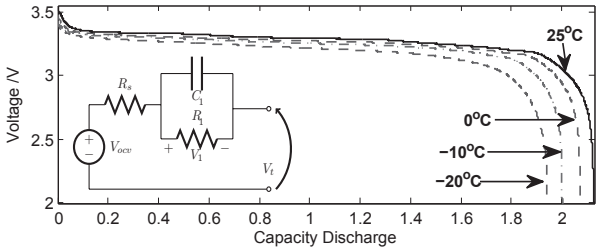

Fig. 1. Relation between Temperature, OCV and capacity, (inset) single R-C equivalent circuit representation of electrical dynamics

A. Electrical Model

Over the decades, much effort has been expended in developing phenomenological models of the electrical dynamics. The more complex models are based on concentration theory, first proposed by Doyle, Fuller and Newman in [8]. Models so derived are hard to parameterize [9], [10], have notable memory requirements and, are computational intensive. On the other hand, equivalent circuit models have been widely adopted in literature and in practice [11], [12].

In this work, owing to its simplicity, the equivalent circuit model (Fig. 1(inset)) whose dynamics is described by Eqn. (1) is utilized. Note that the system that Eqn.(1) describes is one of a Linear Parameter Varying system wherein the parameters are schedule based on the state of charge, z, and the cell temperature T.

$$\underbrace{\begin{bmatrix}\dot{z}\\ \dot{V}_1\end{bmatrix}}_{x_{el}} = \underbrace{\begin{bmatrix}0 & 0\\ 0 & -\dfrac{1}{R_1(z,T)C_1(z,T)}\end{bmatrix}}_{A_{el}}\begin{bmatrix}z\\ V_1\end{bmatrix} + \underbrace{\begin{bmatrix}-\dfrac{1}{3600\cdot C_b(T)}\\ -\dfrac{1}{C_1(z,T)}\end{bmatrix}}_{B_{el}} I$$

$$V_t = V_{OCV}(z,T) - V_1 - R_s(z,T)I \tag{1}$$

where z is the state of charge (SOC) of the cell; C_b, the temperature dependent capacity of the cell; V_t is the terminal voltage of the cell and V_{OCV} is the relation between SOC, Open Circuit Voltage (OCV) and temperature.

Figure 1 presents the OCV against ampere-hours discharged. It is observed that as temperature decreases, capacity C_b[1] decreases.

The electrical model of the Li-cell is parameterized in manner similar to that described in [13]. Space constraints dictate that the parametrization technique, model parameters and inferences from them are omitted.

B. Thermal Model

The thermal model developed in [14] that assumes uniform heat generation along the radius of the cell is taken to represent the thermal dynamics in this study. The model of the thermal dynamics when expressed in terms of the core (T_c), surface (T_s), ambient (T_∞) temperatures and rate of heat generation (q) is represented as

$$\begin{aligned}\dot{x}_{th} &= A_{th}x_{th} + B_{th}u_{th}\\ y_{th} &= C_{th}x_{th} + D_{th}u_{th}\end{aligned} \tag{2}$$

where the states represent temperature gradient across the radius ($\bar{\gamma}$) and average temperature ($\bar{T}$); $x_{th} = [\bar{T}\ \bar{\gamma}]^T$, $u_{th} = [q\ T_\infty]^T$ and $y_{th} = [T_c\ T_s]^T$. System matrices A_T, B_T, C_T, and D_T are defined as follows:

$$\begin{aligned}A_{th} &= \begin{bmatrix}\frac{-48\alpha h}{R(24k_{th}+Rh)} & \frac{-15\alpha h}{24k_{th}+Rh}\\ \frac{-320\alpha h}{R^2(24k_{th}+Rh)} & \frac{-120\alpha(4k_{th}+Rh)}{R^2(24k_{th}+Rh)}\end{bmatrix}\\ B_{th} &= \begin{bmatrix}\frac{\alpha}{k_{th}V_b} & \frac{48\alpha h}{R(24k_{th}+Rh)}\\ 0 & \frac{320\alpha h}{R^2(24k_{th}+Rh)}\end{bmatrix}\\ C_{th} &= \begin{bmatrix}\frac{24k_{th}-3Rh}{24k_{th}+Rh} & -\frac{120Rk_{th}+15R^2h}{8(24k_{th}+Rh)}\\ \frac{24k_{th}}{24k_{th}+Rh} & \frac{15Rk_{th}}{48k_{th}+2Rh}\end{bmatrix}\\ D_{th} &= \begin{bmatrix}0 & \frac{4Rh}{24k_{th}+Rh}\\ 0 & \frac{Rh}{24k_{th}+Rh}\end{bmatrix}\end{aligned} \tag{3}$$

where k_{th}, h and ρ are the thermal conductivity, convection coefficient and bulk density, α, the thermal diffusivity is defined as the ratio of k_{th} to the heat capacity, c_p.

The rate of heat generation is defined as

$$q = I^2R_s(z,\bar{T}) + \frac{V_1^2}{R_1(z,\bar{T})} \tag{4}$$

The parameters of the thermal model, thermal properties of the cell and the environment such as conductivity and convection, are not significantly influenced by temperature variations; this affords us the option of adopting the values presented in [14] without change.

C. Model Validation

To validate the models described in the sections afore, a 26650 LFP cell was instrumented with a thermocouple in its center cavity and was excited with square pulses whose duty-cycle was set to 50%, charging and discharging currents were set at five and 10 amperes. The frequency of current was set to 1Hz and measurements of terminal voltage, current, surface and core temperature were collected at the rate of 100Hz. The measured current was fed to both the electrical and thermal models and the estimated terminal voltage, surface and core temperatures are charted in Fig. 2.

From Fig. 2(a) it is noted that the rms. error in estimating the terminal voltage is less than 50mV. Much of the large errors in estimation of terminal voltage is incident with changes in current direction. The most likely reasons are — (a) while the model is able to capture the steady state values, it has deficiencies in mimicking the transient response; (b) inherent delays in simulating a continuous system in discrete time.

Figure 2(b) presents the outcome of simulating the thermal model. The input to the thermal model was computed using the electrical model parameters and states. Upon inspection, it is possible to conclude that the thermal model is able to predict the surface and core temperatures to within the

[1]The magnitude of current that completely discharges a fully charged cell one hour is denoted as 1C. In the context of this work, the capacity is measured by drawing a current equal to C/20.

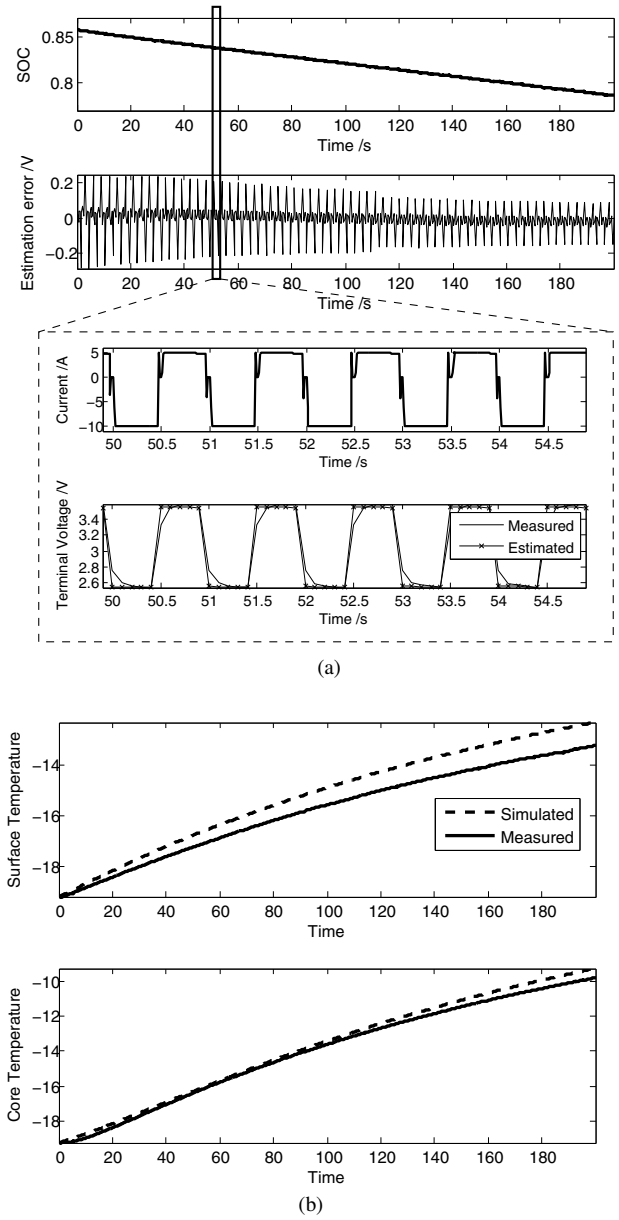

Fig. 2. Model Validation: (a) Prediction of Terminal Voltage (b) Predicting Surface and Core temperatures

accuracy of the T-junction thermocouples (0.5°C).

III. Problem Formulation

The objective of this work is to warm the cell in an energy efficient manner until the desired power can be drawn from the cell. To this end, based on electrochemical considerations, the profile of input current is chosen as a sequence of bi-directional pulses recurring at a certain frequency.

To keep the complexity of the problem tractable, each period of the current is stipulated to have just one sign change of current and the duty cycle is pre-set to equal 50%[2].

The electrical and thermal behavior of the cell are functions of its operating conditions and internal states. The problem of deciding the peaks of the charging and discharging portions of the period is formulated as a linearized receding finite horizon optimization problem and described in this section.

For simplicity in expressions, in the following, it is assumed that each period of the current is spread over only two samples. A more general case is easily derived by scaling the appropriate variables.

A. Characterizing the Current Profile

Exploiting the inherent feedback between the thermal and electrical sub-systems[3], at each instant k, for a prediction horizon of length $2N$ samples, the problem of deciding the magnitude of pulses is computed by solving the following problem **P1**:

$$\min_u J = -[\bar{T}_{k+2N+1} - \bar{T}_{k+1}] + \beta|z_{k+2N+1} - z_{k+1}|$$

s.t. :

$$\left.\begin{aligned} x_{th,k+1} &= A^d_{th}x_{th,k} + B^d_{th}v_{th,k} \\ y_{th,k} &= C^d_{th}x_k + D^d_{th}v_{th,k} \\ v_{th,k} &= [u_k^2 R_{s,k}; T_{\infty,k}] \end{aligned}\right\} \quad (5a)$$

$$\left.\begin{aligned} |u_i| &\le |I_d(\bar{T})|,\ \forall i \in \{1,3,\ldots,2N-1\} \\ |u_i| &\le |I_c(\bar{T})|,\ \forall i \in \{2,4,\ldots,2N\} \\ |u_i| &\ge |u_{i+1}|,\ \forall i \in \{1,3,\ldots,2N-1\} \end{aligned}\right\} \quad (5b)$$

$$\left.\begin{aligned} x_{el,k+1} &= A^d_{el,k}x_{el,k} + B^d_{el,k}u_k \\ y_{el,k} &= C^d_{el,k}x_{el,k} + D^d_{el,k}u_k + G^d_{el,k} \end{aligned}\right\} \quad (5c)$$

$$\left.\begin{aligned} V_{t,i} &\le V_{max},\ \forall i \in \{k+1,\ldots,k+2N\} \\ -V_{t,i} &\le -V_{min},\ \forall i \in \{k+1,\ldots,k+2N\} \end{aligned}\right\} \quad (5d)$$

$$-z_i \le -\bar{z},\ \forall i \in \{k+1,\ldots,k+2N+1\} \quad (5e)$$

where $G^d_k = V_{ocv}(z_{k-1})C^d_k(1)z_{k-1}$ and $u = [u_1,\ldots,u_{2N}]'$.

The cost function of **P1** strikes a compromise between total increase in the cell's average temperature and penalized loss in state of charge[4] over the entire prediction horizon. Eqns. (5a) and (5d) describe the equality constraints on the temperature and electrical model dynamics in which a superscript 'd' indicates the discrete version of the variable. Eqns. (5b) impose restriction on the magnitude of the current pulses; the maximum current that can be delivered(I_d)/absorbed(I_c) is captured as a function of average cell temperature. For safety concerns, Li-ion cells are, in practice set to operate within a set window of terminal voltage, $[V_{min}, V_{max}]$; Eqns. (5c) enforce constraints on terminal voltage. Finally, Eqn. ((5d) enforces the SOC at any instant to be above a minimum value of $\bar{z}$.

By substituting the model dynamics into the cost and by iteratively aggregating the constraints, Problem **P1** can be

[2]A variable duty cycle formulation is possible but is not trivial to solve.

[3]The power capability of a Li-ion cell is possibly limited by two factors – (1) temperature dependence of material properties, (2) large concentration gradients across the electrodes; notably , the latter reason is to a large extent impacted by the former.

[4]Loss in state of charge, in this context is interpreted as a loss in internal energy storage.

recast into a standard optimization problem **P2**

$$\min_u J = -\|u\|_W^2 + \beta' \sum_j u_j$$

$$\text{subject to : } \Psi u \leq \Upsilon$$
$$|u_i| \leq |I_d(\bar{T})|, \forall i \in \{1, 3, \ldots, 2N-1\}$$
$$|u_i| \leq |I_c(\bar{T})|, \forall i \in \{2, 4, \ldots, 2N\}$$
$$|u_i| \geq |u_{i+1}|, \forall i \in \{1, 3, \ldots, 2N-1\}$$

where $W > 0$, and Ψ and Υ are matrices that incorporate the lifted system dynamics and other constraints on states.

P2 is one of concave minimization over a convex polyhedron; solutions to such problems lie at the vertices of the polyhedron [15]. In this work a vertex enumeration based method is adopted to solve **P2**.

IV. Simulation and Discussion

In this section, the proposed Pulsed Current Method (PCM) is simulated with the models described in section II.

A. Simulation Setup

The augmented electro-thermal model is nonlinear in input and output; the proposed algorithm is implemented using local linear models and is simulated in the MATLAB/Simulink environment using a custom vertex enumerator.

In implementing the pulsed-current algorithm, simplifications and variable values were chosen as follows. The cell operating voltage bounds were set at $[2, 3.6]$; the frequency of the pulse train was set to 10Hz based on electrochemical considerations [16] and the model was simulated at Nyquist frequency.

The time constant of the thermal dynamics of the cell under consideration is in the order of tens of minutes. Thus, the increase in temperature as a result of applying one period of current (at 10Hz) may not be measurable by the thermocouple. For this reason, in this study, the problem of current magnitude determination is solved in blocks.

Periods in the prediction horizon are binned into blocks, with each block consisting of a pre-set number of pulse periods; the prediction horizon is then described by the number of blocks. The optimization problem as formulated earlier is modified to enforce the constraint that every period in each block is identical. This correction also has the added benefit of providing more measurement samples for online adaptation of models and estimation.

The simulated 26650 A123 cell is assumed to be a part of a pack that consists of 60 cells in series and four cells in parallel. Limits on the maximum deliverable current were set by factoring in manufacturers specifications (Table I) and the standards proposed by USABC [17]. Note that the specifications provided in Table I are for continuous discharge. For pulsed currents the current limits are set as follows

$$I_c(T) = \begin{cases} 2.9A & T \leq 0^oC \\ \min\{e^{-\frac{12730.35}{(273+T)}+47.7}, 150\}A & 0^oC < T < 60^oC. \end{cases}$$

The discharge current limit (I_d) is set to a constant value of 150A. The power capability is computed as that which can be drawn from the cell for a period of 10 seconds without violating voltage and SOC constraints.

TABLE I

Manufacturers specifications for A123 26650 cells

Direction	Temperature	Continuous Current
Charge	0–20^{o}C	3A
Charge	20–50^{o}C	10A
Discharge	-30–60^{o}C	60A

B. Results and Discussion

In what follows, the framework of PCM as set-up above is simulated for different value of $\beta \in [0.5, 0.7]$ and the results are compared against the following cases – (1) the limiting case when $\beta = 0$ and (2) the case of maximum permissable continuous discharge. In the latter case, the current that is drawn ensures that the terminal voltage is pegged at V_{min}, and is the solution of the minimum time problem for battery warm-up; this operation is labeled Constant Voltage Method (CVM).

1) Baseline : Comparing PCM & CVM: Figures 3 and 4 present down-sampled results (one in 19 samples) of simulating the electro-thermal model using the proposed reference current generation algorithm and CVM using power (P_{dmd}) as terminal constraint. The optimization parameters are $\beta = 0$, $P_{dmd} = 100$W at $SOC_0 = 0.6$, ambient temperature set to -20^oC and natural cooling condition ($h = 5\,W/m^2K$) and prediction horizon length $N = 1$.

From Fig. 3 it is evident that for PCM, voltage constraints are active during discharge and that current is constrained while charging, pointing in the direction of minimizing external energy stored. The trajectory of estimated of power capability is presented in Fig. 4 and possess an interesting shape.

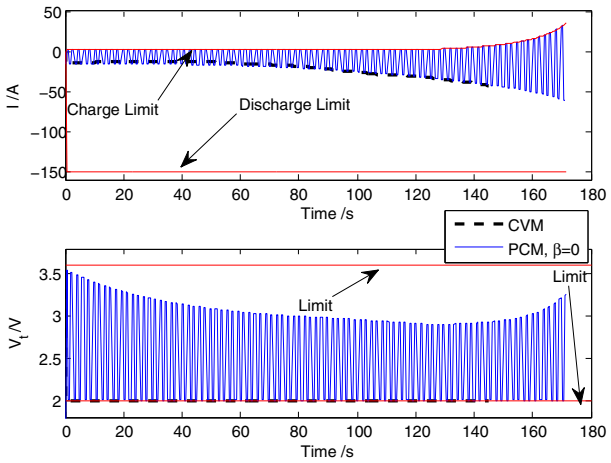

Fig. 3. Down-sampled simulated trajectory of (down-sampled by 19) voltage and current using PCM ($\beta = 0$)

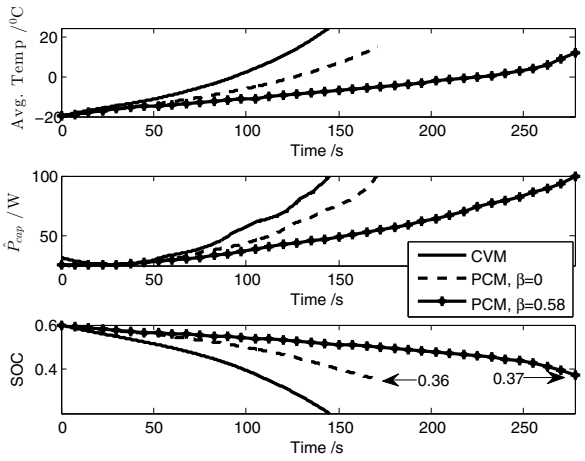

Fig. 4. Down-sampled simulated trajectory of average temperature and power capability using PCM and CVM; $SOC_0 = 0.6$, $P_{dmd} = 100$W, $h = 5W/m^2K$

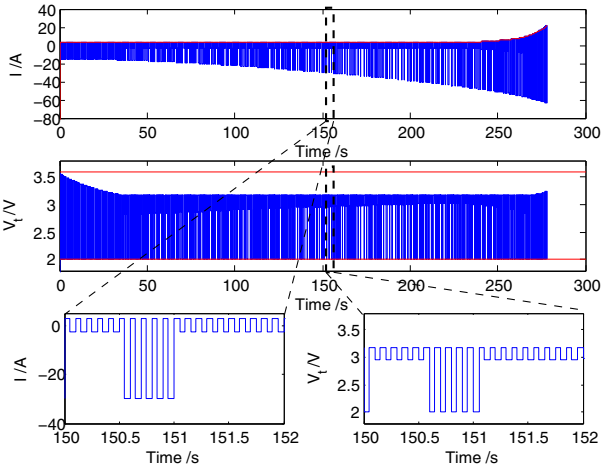

Fig. 5. Down-sampled simulated trajectory of (down-sampled by 19) voltage and current using PCM, $\beta = 0.58$

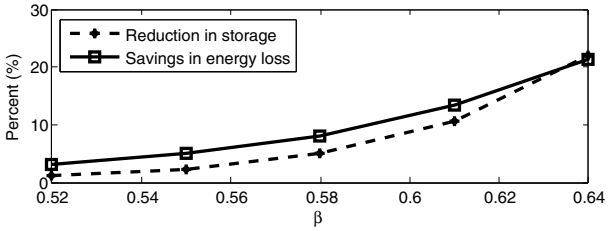

Fig. 6. Results on increasing penalty on energy loss as percent of when no penalty is applied.; initial conditions – natural convection with $P_{dmd} = 100W$, ambient temperature : -20^oC, initial SOC : 0.6, prediction length : 1 block of 5 periods

The almost-convexity of the power capability trajectory can be explained as follows. The current drawn from the cell in the initial period is predominantly negative; the biased current increases the voltage across the R-C pair as the simulation progresses. According to the equivalent circuit model, the increased 'polarization' adversely impacts the power capability (calculated based on the method described in [18]). As temperature increases, the parameters of the gain scheduled model change to reflect the decreasing resistance and time constants, thereby reducing rate of increase of 'polarization' and assisting in drawing more power during discharge pulses.

The PCM and CVM simulation results (Fig. 4) highlight some of the key differences (aggregated in Table II) between the two methods. Since the maximum permissable constant current is drawn from the cell in CVM (discharge current limits being larger in magnitude than charging current constraint), the rise in battery temperature is faster and the risk of adverse side reactions at the anode is minimized. However, this comes at the cost of external storage – warranting almost twice as much external storage as compared to PCM. The increased polarization voltage can be interpreted as either the anode (closest to the separator) tethering on Li depletion and large gradients across the electrolyte. Large gradients across the electrode can result in the propagation of stress cracks and adversely influence the life of cells [19].

2) Penalizing energy loss: The energy removed from the cell over the course of the warm-up process, in this study is assumed to be stored in external storage elements such as ultra-capacitors. As formulated, the value of β in the cost can be use to regulate the amount of energy dissipated as heat. Figure 5 depicts the trajectory of current and voltage for the specific case when $\beta = 0.58$. Note that unlike the case when $\beta = 0$, the trajectory of voltage does not always hit the lower limit of 2V. The reason for this behavior is related to the perceived ability to increase temperature at the expense of SOC which in turn is a function of local model parameters and the value of internal polarization. The evolution of power capability and average temperature for this particular case is shown in Fig. 4.

Figure 6 documents the savings in energy for different values of β and also the reduction in sizing requirement of the external storage elements. Inspecting Fig. 6, it it evident that increasing the value of β can reduce energy expenditure and external sizing by as much as 20%. This increased efficiency of operation does however come at a price.

Figure 7 presents a comparison between the increase in warm-up efficiency and time taken to be able to deliver the desired power. Evidently, in order to increase the efficiency of operation, the implicit penalty on operation time is quite significant.

3) Increasing the prediction horizon: In simulating the results presented thus far, the prediction horizon was set to be a single block consisting of five pulses. In the context of predictive control, longer prediction horizons are known

TABLE II
COMPARISON BETWEEN PCM* AND CVM, KEY INDICES

Method	Oper. Time	z_{store}	T_{final}	z_{loss}
PCM ($\beta = 0$)	172s	0.13	17.5^{o}C	0.11
PCM ($\beta = 0.58$)	278s	0.12	12.25^{o}C	0.10
CVM	143s	0.23	24.3^{o}C	0.15

*1 block with 5 periods

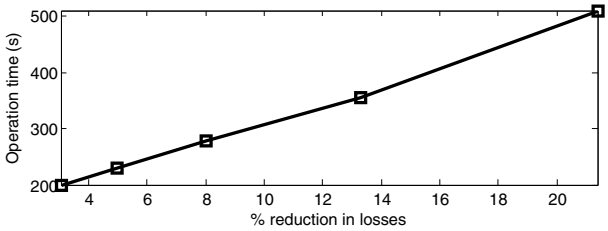

Fig. 7. Comparison between increased efficiency and warm-up operation time

TABLE III

COMPARING THE IMPACT OF PREDICTION HORIZON BASED ON KEY INDICES*

Index \ Prediction Length	1	2	3
SOC_{loss}	1	0.99	0.98
External Storage	1	0.99	0.97
Terminal Time	1	1.01	1.03
Computational Time	1	35	107

* Entries normalized wrt. results when prediction length is one block

to produce better approximations of the global optimal solution. In this application, owing to the linearized MPC implementation, the prediction horizon cannot be taken to be arbitrarily large without incurring errors resulting from model linearization.

To investigate the influence of prediction horizon on the optimal solution trajectory, an iterative test was performed[5] wherein the length of the prediction horizon was increased incrementally; results of which are presented in Table III. The other parameters of the simulation were : $P_{dmd} = 50W$, $h = 5W/m^2K$ and $\beta = 0.57$.

The data presented in Table III, as expected, indicates that given the same penalty on loss in energy, increasing the length of the prediction horizon decreases the total energy lost; this however does come at the expense of computational time. In fact, there appear to be a quadratic relation between decrease in loss and total operation-time. Comparing the effective increase in savings and the increase in computational and operation time, a case for the use of prediction horizon of length one block can be made.

V. CONCLUSION

In this work, a Li-ion battery warm-up strategy that increases the cell temperature to meet power demand in an energy efficient method is described. The shape of current drawn from the cell was set to be bi-directional pulses to minimize 'polarization' and reduce damage to electrodes. Magnitude of the pulses were determined by solving a constrained optimization problem. From simulations based on models of an A123 26650 cell, it is noted it is possible to reduce energy lost as heat by as much as 20%. A future work will study and report the impact of the proposed technique on a real battery.

[5]Simulations were performed on a computer powered by an Intel i5-2500 quad-core processor with 16GB of ram and running Windows 7 with parallelization enabled.

ACKNOWLEDGEMENTS

The authors would like to acknowledge the financial assistance provided by the U.S. Army Tank Automotive Research, Development and Engineering Center (TARDEC) and the Automotive Research Center (ARC).

REFERENCES

[1] L. Liao, P. Zuo, Y. Ma, X. Chen, Y. An, Y. Gao, and G. Yin, "Effects of temperature on charge/discharge behaviors of lifepo4 cathode for li-ion batteries," *Electrochimica Acta*, vol. 60, no. 0, pp. 269 – 273, 2012.

[2] S. Zhang, K. Xu, and T. Jow, "Low temperature performance of graphite electrode in li-ion cells," *Electrochimica Acta*, vol. 48, no. 3, pp. 241 – 246, 2002.

[3] T. M. Bandhauer, S. Garimella, and T. F. Fuller, "A critical review of thermal issues in lithium-ion batteries," *J. Electrochem. Soc*, vol. 158, no. 3, pp. R1–R25, 2011.

[4] M. C. Smart and B. V. Ratnakumar, "Effect of cell design parameters on lithium plating in lithium-ion cells," *Journal of the Electrochemical Society*, vol. 158(4), pp. 279–389, 2011.

[5] Z. G. Lei and C. N. Zhang, "Research development on heating system of evs battery pack," *Advanced Materials Research*, vol. 284-286, pp. 1947–1951, 2011.

[6] Y. Ji and C. Y. Wang, "Heating strategies for li-ion batteries operated from subzero temperatures," *Electrochimica Acta*, vol. 107, no. 0, pp. 664 – 674, 2013.

[7] Y. Ji, Y. Zhang, and C.-Y. Wang, "Li-ion cell operation at low temperatures," *Journal of The Electrochemical Society*, vol. 160(4), pp. 636–649, 2013.

[8] M. Doyle, T. F. Fuller, and J. Newman, "Modeling of galvanostatic charge and discharge of the lithium/polymer/insertion cell," *Journal of Electrochemical Society*, vol. 140(6), pp. 1526–1533, 1993.

[9] A. P. Schmidt, M. Bitzer, rpd W. Imre, and L. Guzzella, "Experiment-driven electrochemical modeling and systematic parameterization for a lithium-ion battery cell," *Journal of Power Sources*, vol. 195, no. 15, pp. 5071 – 5080, 2010.

[10] J. Forman, S. Moura, J. Stein, and H. Fathy, "Genetic parameter identification of the doyle-fuller-newman model from experimental cycling of a lifepo4 battery," in *American Control Conference (ACC), 2011*, pp. 362–369, 2011.

[11] L. Lam, P. Bauer, and E. Kelder, "A practical circuit-based model for li-ion battery cells in electric vehicle applications," in *Telecommunications Energy Conference (INTELEC), 2011 IEEE 33rd International*, pp. 1 –9, oct. 2011.

[12] K. A. Smith, C. D. Rahn, and C.-Y. Wang, "Control oriented 1d electrochemical model of lithium ion battery," *Energy Conversion and Management*, vol. 48, no. 9, pp. 2565 – 2578, 2007.

[13] X. Lin, H. E. Perez, S. Mohan, J. B. Siegel, A. G. Stefanopoulou, Y. Ding, and M. P. Castanier, "A lumped-parameter electro-thermal model for cylindrical batteries," *Journal of Power Sources*, vol. 257, no. 0, pp. 1 – 11, 2014.

[14] Y. Kim, S. Mohan, J. B. Siegel, A. G. Stefanopoulou, and Y. Ding, "The estimation of temperature distribution in cylindrical battery cells under unknown cooling conditions," *Transactions on Control System Technology*, 2014. To appear.

[15] R. T. Rockafellar, *Convex analysis*, vol. 28. Princeton university press, 1997.

[16] S. Tippmann, D. Walper, L. Balboa, B. Spier, and W. G. Bessler, "Low-temperature charging of lithium-ion cells part i: Electrochemical modeling and experimental investigation of degradation behavior," *Journal of Power Sources*, vol. 252, no. 0, pp. 305 – 316, 2014.

[17] T. I. N. Laboratory, *Battery Test Manual For Plug-In Hybrid Electric Vehicles*. U.S. Department of Energy Vehicle Technologies Program, 2 ed., December 2010.

[18] Y. Kim, S. Mohan, J. B. Siegel, and A. G. Stefanopoulou, "Maximum power estimation of lithium-ion batteries accounting for thermal and electrical constraints," in *DSCC*, 2013.

[19] K. Zhao, M. Pharr, J. J. Vlassak, and Z. Suo, "Fracture of electrodes in lithium-ion batteries caused by fast charging," *Journal of Applied Physics*, vol. 108, no. 7, pp. 073517–073517–6, 2010.